Structure, Isomerism, and Ligand Dynamics in Dioxouranium(VI) Complexes

Zoltán Szabó, Wenche Aas, and Ingmar Grenthe*

Department of Chemistry, Inorganic Chemistry, Royal Institute of Technology (KTH), S-100 44 Stockholm, Sweden

Received July 2, 1997[⊗]

The ligand exchange reactions in complexes of the type $UO_2LF_n(H_2O)_{3-n}$, where $n = 1-3$ and L is one of the bidentate ligands picolinate (pic), oxalate (ox), carbonate, and acetate (ac), UO_2L_2F (L = picolinate or oxalate), have been investigated by using an array of $^{19}F-$, $^{13}C-$, $^{17}O-$, and ^{1}H-NMR techniques. The rates of exchange were sufficiently low to allow the identification of isomers, which are those expected for a pentagonal bipyramid coordination geometry, with the "yl" oxygens in the apical positions. All ligand exchange reactions were independent of the concentration of free ligand. Two different fluoride exchange pathways were identified, *intermolecular* exchange between coordinated and free fluoride and *intramolecular* exchange between different fluoride sites within a given complex. The intramolecular exchange reaction in $UO_2(pic)F_3^{3-}$ was shown to be a result of opening/closing of the chelate ring, equivalent to a site exchange between the two "edge" fluorides. Dissociation of acetate is the major factor determining the intramolecular fluoride exchange reactions in $UO_2(ac)F_3^{2-}$. In this same way the broad ^{19}F-NMR peaks for $UO_2LF_2(H_2O)^{2-}$ and $UO_2LF(H_2O)_2^{-}$ are a result of a comparatively slow exchange between coordinated and bulk water. At pH > 6 $UO_2(ox)F(H_2O)_2^{-}$ forms a hydroxide-bridged dimer $(UO_2)_2(ox)_2F_2(OH)_2^{4-}$, which exists in two isomeric forms.

Introduction

The linear dioxoactinoid(VI) ion, *e.g.*, UO_2^{2+} has an unusual coordination geometry with two substitution-inert "yl" oxygen atoms forming the apices in a pentagonal or hexagonal bipyramid with the substitution-labile ligands in, or close to, the plane perpendicular to the linear axis.[1−3] Most structural information is based on data from X-ray investigations of solid compounds, while the information on aqueous species is inferred from the constitution of complexes, determined by equilibrium analysis and/or spectroscopic techniques. There is also some direct structure information based on large-angle X-ray scattering[4,5] or EXAFS data.[3,6] In this study the coordination geometry of dioxouranium(VI) complexes was determined by identifying isomers in solution, *i.e.*, extending the classical Werner method to labile complexes. Following Werner this was done by varying the donor atoms and the denticity of the ligands used. The possibility of identifying isomers in rapid equilibrium with one another depends on the rates of *inter*- and *intramolecular* exchange reactions between coordinated and free ligand(s), and the sensitivity of the physical parameter used to distinguish the isomers, in our case the NMR chemical shift differences of nuclei in different surroundings. The rate of exchange of a given ligand depends on all dynamic events in the coordination sphere. This makes it possible to use one NMR-active donor atom, in this case ^{19}F, as a probe to study the dynamics of other ligands which are not easily studied directly, *e.g.*, water.

In our previous studies[7,8] of the binary $UO_2^{2+}-F^-$ system in aqueous solution we observed that the exchange processes between the various complexes were so slow on the ^{19}F-NMR chemical shift scale that both one- and two-dimensional magnetization transfer experiments could be used to study the equilibrium kinetics at −5 °C, but not slow enough to observe separate fluoride peaks from the different chemical environments in the isomers of $UO_2F_n(H_2O)_{5-n}^{2-n}$ (for $n = 2$ and 3). Our previous study[8] indicated that coordinated water had a large influence on the rate of exchange of the fluoride ligands. The mobility of bidentate ligands is smaller than that of water. Hence, the investigation of ternary complexes with no coordinated water molecules or a small number of them might provide insight both on isomer formation and on *inter*- and *intramolecular* ligand exchange mechanisms. In order to explore this we investigated different $UO_2^{2+}-F^-L^{n-}$ systems, containing 0, 1, or 2 coordinated water molecules. The ligand L^{n-} is a symmetric bidentate ligand, oxalate or carbonate, an unsymmetric bidentate ligand like picolinate, or the weakly coordinated acetate.

Chemical Approach. All schemes will be based on the assumption of a pentagonal bipyramid geometry for the various complexes. The experimental data confirmed that alternatives, *e.g.*, a hexagonal bipyramid geometry, could be excluded. Scheme 1 shows a cartoon of the complex $UO_2F_n(XY)(H_2O)_{3-n}$, ($n = 1-3$). The charges have been omitted for simplicity. In oxalate and carbonate, X = Y = O; in picolinate, X = O and Y = N. The complex is located in a solvent cage, and exchange reactions may occur between ligands *within* the complex (*intramolecular* exchange reactions) and/or between the coordinated ligands and the free ligand. If $n = 3$ and the exchange reactions are sufficiently slow, one should observe two different fluoride sites for the symmetrical and three for the unsymmetrical ligands in the case of a pentagonal bipyramid coordina-

* Author to whom correspondence should be addressed.

⊗ Abstract published in *Advance ACS Abstracts,* October 1, 1997.

(1) Clark, D. L.; Hobart, D. E.; Neu, M. P. *Chem. Rev.* **1995**, *95*, 25.
(2) Wells, A. F. *Structural Inorganic Chemistry*, 5th ed.; Clarendon Press: Oxford, 1984.
(3) Allen, P. G.; Bucher, J. J.; Clark, D. L.; Edelstein, N. M.; Ekberg, S. A.; Gohdes, J. W.; Hudson, E. A.; Kaltsoyannis, N.; Lukens, W. W.; Neu, M. P.; Palmer, P. D.; Reich, T.; Shuh, D. K.; Tait, C. D.; Zwick, B. D. *Inorg. Chem.* **1995**, *34*, 4797.
(4) Åberg, M.; Ferri, D.; Glaser, J.; Grenthe, I. *Inorg. Chem.* **1983**, *22*, 3981.
(5) Åberg, M.; Ferri, D.; Glaser, J.; Grenthe, I. *Inorg. Chem.* **1983**, *22*, 3986.
(6) Allen, P. G.; Shuh, D. K.; Bucher, J. J.; Edelstein, N. M.; Reich, T.; Denecke, M. A.; Nitsche, H. *Inorg. Chem.* **1996**, *35*, 784.
(7) Szabó, Z.; Glaser, J. *Magn. Reson. Chem.* **1995**, *33*, 20.
(8) Szabó, Z.; Glaser, J.; Grenthe, I. *Inorg. Chem.* **1996**, *35*, 2036.

S0020-1669(97)00817-3 CCC: $14.00

Scheme 1

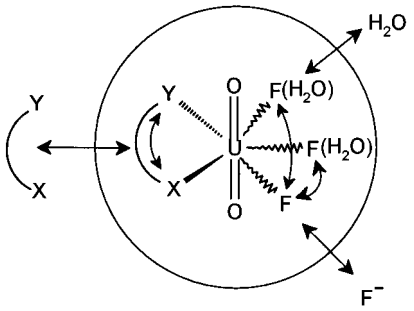

tion geometry. If the geometry is hexagonal bipyramid, there are four and two isomers, respectively, each with three different fluorine sites for both the symmetrical and the unsymmetrical ligand.

Experimental Section

Chemicals and Solutions. A uranium(VI) perchlorate stock solution was prepared as described earlier.[9] NaF, Na_2CO_3, $Na_2(C_2O_4)$, CH_3COONa, picolinic acid, and 4-nitro- and 4-(3-pentyl)picolinic acids were used to prepare the various test solutions. The syntheses of 4-(3-pentyl)-picolinate and 4-nitropicolinate are described elsewhere.[10,11] The experiments were made in 1.0 M $NaClO_4$ ionic medium. The pH was measured and recalculated to concentrations using the method suggested by Irving et al., as described before.[8] Solutions of $HClO_4$ and NaOH were used to vary pH. ^{17}O-NMR measurements were performed by using ^{17}O-enriched (about 4%) samples. The enrichment of the "yl" oxygens of UO_2^{2+} was made as described previously[12] using ^{17}O-enriched water (Isotec Inc 37.8% ^{17}O). ^{13}C-NMR measurements were made using solutions of ^{13}C-enriched $Na_2(C_2O_4)$ (Isotec Inc. 99.2% ^{13}C) and Na_2CO_3 (Stohler Isotope Chemical 99.3% ^{13}C).

NMR Measurements. The NMR spectra were recorded on Bruker AM400 and DMX500 spectrometers at −5 °C if nothing else is mentioned. D_2O solutions (5%) were used in the locked mode. Solutions in 99% CD_3OD were used for measurements at lower temperatures. The temperature control/measurement technique was the same as before;[8] however, temperatures below −5 °C were checked from the chemical shifts of methanol.[13] The test solutions were measured in 5 mm (for ^{19}F and ^{1}H) or 10 mm (for ^{17}O and ^{13}C) NMR tubes with Teflon inserts for the acid solutions. The ^{19}F-NMR spectra recorded at 376.4 or 470.5 MHz were referenced to an aqueous solution of 0.01 M NaF in 1 M $NaClO_4$ (pH = 12) at 25 °C, and the ^{17}O-NMR spectra (at 54.2 MHz) to external tap water at 25 °C. ^{13}C-NMR spectra (at 100.6 or 125.7 MHz) and ^{1}H-NMR spectra (at 400.1 or 500.1 MHz) were referenced to the methyl signal of sodium 3-(trimethylsilyl)-propionate-d_4 at 25 °C. Selective inversion transfer experiments were performed using a DANTE pulse train.[14] The line widths were determined by fitting a Lorentzian curve to the experimental signal using standard Bruker software. In some cases deconvolution of overlapping peaks was made using the WIN-NMR program, which yielded both the integrals and the line widths.[15]

Data Treatment and Dynamic Calculations. The applications of different dynamic NMR methods are very well documented in the literature, and only a short summary of the ones used here is given. In the slow-exchange regime separate peaks for the exchanging sites were observed in the NMR spectra. We used one- and two-dimensional magnetization transfer experiments, as detailed in the literature,[16−18] which provide information on the exchanging system if the rate is too slow to have an effect on the line shape (but comparable to the reciprocal value of the longitudinal relaxation time, $1/T_1$, of the exchanging species). The rate constants were obtained by inverting one of the peaks using a 180° selective pulse and then observing all of the peaks by a delayed (t) 90° hard pulse. The desired kinetic information was calculated from the time dependence of the signal intensities by a nonlinear fitting procedure based on the Bloch−McConnell equations, modified for the transfer of magnetization by chemical exchange,[16,19] eq 1, where $M_{i(t)}$ and $M_{i(\infty)}$ are the z-magnetiza-

$$\mathrm{d}[M_{i(t)} - M_{i(\infty)}]/\mathrm{d}t = R[M_{i(t)} - M_{i(\infty)}] \quad (1)$$

tion of site i at time t and at equilibrium, respectively. R is the rate matrix with the rate constants k_{ij} ($i \neq j$) as off-diagonal elements, and the sum of the exchange rates k_{ji} and the relaxation rates $(1/T_1)_i$ ($j \neq i$) as the diagonal elements For exchange between more than two sites, eq 1 is written as

$$M_{i(t)} = M_{i(\infty)} + \exp(Rt)[M_{i(t)} - M_{i(\infty)}] \quad (2)$$

The solution after diagonalization of R by means of $R = X\Lambda X^{-1}$ (X is the eigenvector matrix, X^{-1} its inverse, and Λ the diagonal eigenvalue matrix) is

$$M_{i(t)} = M_{i(\infty)} + \sum_{j=1}^{n} c_{ij} \exp(-\lambda_j t) \quad (3)$$

where

$$c_{ij} = X_{ij} \sum_{k=1}^{n} (X^{-1})_{jk}[M_{k(0)} - M_{k(\infty)}] \quad (4)$$

λ_j are the elements of Λ, and $M_{i(0)}$ is the initial magnetization of the site i.

When the exchange rate is fast enough to affect the line shape, but still too slow on the chemical shift scale to result in a coalescence of peaks, the pseudo-first-order rate constants may be calculated from the line widths of exchanging species:

$$\pi\Delta\nu_{1/2}(i) = \pi\Delta\nu^{\circ}_{1/2}(i) + \sum_{j=1}^{n} k_{ij} \quad (5)$$

where $\Delta\nu^{\circ}_{1/2}(i)$ is the nonexchange line width for the ith species and k_{ij} the pseudo-first-order rate constant for the chemical exchange process between sites i and j.

If the exchange rate is fast on the chemical shift scale, as a result of overlapping or coalescence of the peaks, only one peak is observed in the spectrum. The band shape can then be calculated from the individual chemical shifts and the relative populations of the exchanging species by a matrix formalism suggested by Reeves and Shaw.[20] In this case the quadratic rate matrix contains the linear combination of pseudo-first-order rate constants between the sites involved in the exchange. Then the determination of the kinetic parameters is based on a comparison between the measured and the calculated spectra.

Results and Discussion

Constitution. The stoichiometry and equilibrium constants for the complexes (see Supporting Information, T1) were determined by standard solution chemical methods as described

(9) Ciavatta, L.; Ferri, D.; Grenthe, I.; Salvatore, F. *Inorg. Chem.* **1981**, *20*, 463.
(10) Elman, B.; Högberg, A. G. S.; Moberg, C.; Muhammed, M. *Polyhedron* **1986**, *5*, 1917.
(11) Hoare, J. L.; Cavell, K. J.; Hecker, R.; Skelton, B. W.; White, A. H. *J. Chem. Soc., Dalton Trans.* **1996**, 2197.
(12) Bányai, I.; Glaser, J.; Micskei, K.; Tóth, I.; Zékány, L. *Inorg. Chem.* **1995**, *34*, 3785.
(13) Geet, A. L. V. *Anal. Chem.* **1970**, *42*, 679.
(14) Morris, A. G.; Freeman, R. *J. Magn. Reson.* **1978**, *29*, 433.
(15) WIN-NMR; 950901.0 ed.; Bruker-Franzen Analytik GmbH.
(16) Orrell, K. G.; Šik, V.; Stephenson, D. *Prog. Nucl. Magn. Reson. Spectrosc.* **1990**, *22*, 141.
(17) Sandström, J. *Dynamic NMR Spectroscopy*; Academic Press: London, 1982.
(18) Forsén, S.; Hoffman, R. A. *J. Chem. Phys.* **1963**, *39*, 2892.
(19) Led, J. J.; Gesmar, J. *J. Magn. Reson.* **1982**, *49*, 444.
(20) Reeves, L. W.; Shaw, K. N. *Can. J. Chem.* **1970**, *48*, 3641.

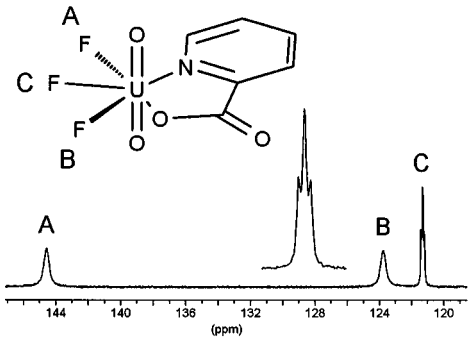

Figure 1. ^{19}F-NMR spectrum showing different peaks of $UO_2(pic)F_3^{2+}$ (pic = picolinate), at −5 °C. The inset shows the fluorine couplings of 37 Hz for F(C).

in a forthcoming communication.[21] Through potentiometric measurements the species UO_2LF_n (n = 1−3) and UO_2L_2F where L = picolinate, cabonate, or oxalate (the charges are left out for simplicity during the whole discussion) were identified. NMR spectra confirm the 5-fold coordination around UO_2^{2+}, and the integral intensities for the different species were in accordance with those expected for the speciation calculated from the stability constants. $UO_2LF(H_2O)_2^-$ and the polynuclear complex $(UO_2)_2L_2F_2(OH)_2^{2-}$ were only observed in the oxalate system, as discussed below. $UO_2(CO_3)_2F^{3-}$ was present in too small a concentration to be observed. Only one of the ternary acetate complexes, $UO_2(ac)F_3^{2-}$, was investigated in detail.

NMR Investigations. Most spectra were recorded at −5 °C, but it was still difficult to detect some signals even at this temperature, because of broadening. There are large ^{19}F-NMR chemical shift differences between the different complexes, and also between different sites within the same complex. NMR peak assignment was made by systematically varying the known analytical total concentrations of the components and calculating the species distribution from the equilibrium constants given in the Supporting Information (T1).

Structure and Dynamics in $UO_2(pic)F_3^{2-}$. Three ^{19}F-NMR signals with approximately the same intensity were observed: two fairly broad (140−145 Hz) independent of free fluoride concentration centered at 144.5 and 123.9 ppm, and one narrower at 121.3 ppm (Figure 1). The latter is a triplet with coupling to the other two fluorides ($^2J_{F,F}$ = 37 Hz). The relatively high chemical shift of the 144.5 ppm signal is probably a result of proximity to the H-6 proton of the pyridine ring. The various fluorides in Figure 1 have been assigned from their chemical shifts and spin−spin couplings. The following set of experiments were carried out in order to explore the mechanisms of bulk and site fluoride exchanges.

1. ^{19}F-NMR inversion transfer experiments in a solution of 5 mM U(VI), 25 mM picolinate, and 100 mM fluoride at pH = 7, where the dominant complex is $UO_2(pic)F_3^{2-}$, were carried out. All three ^{19}F signals in this complex and that of free fluoride (the line width is 3 Hz) were selectively inverted, and the time dependence of their intensities was analyzed by the nonlinear fitting procedure outlined above (cf. Experimental Section). Figure S1 (in the Supporting Information) shows the time dependence of these signals after selective inversion of the edge fluoride signal (F_A). From these experiments the following four processes and their pseudo-first-order rate constants were established: three exchange reactions between free and coordinated fluorides, with rate constants 12.8 ± 0.3 s^{-1} for the edge and 24.4 ± 0.6 s^{-1} for the central fluorides, respectively, and one intramolecular exchange reaction between the two edge fluorides with a rate constant of 301 ± 36 s^{-1}. The magnitude of the latter rate constant shows that this exchange cannot take place via free fluoride; it must be *intramolecular*.

2. Exchange between coordinated and free picolinate will result in a change of surroundings for the two edge fluorides in half of the exchanges. This assertion was tested by magnetization transfer experiments in a solution at the same concentrations and pH as used in the previous experiment. The ^{1}H-NMR spectrum consisted of two sets of signals, one for the coordinated and one for the free picolinate ligand (see Supporting Information, S2). The chemical shift differences were sufficiently large for the use of selective inversion of the protons. An example of magnetization time courses is shown in the Supporting Information (S3). Signals of both coordinated and free ligand were inverted and analyzed simultaneously. The calculated pseudo-first-order rate constant, 4.7 ± 0.2 s^{-1}, was shown to be independent of the concentration of free picolinate. Hence, this reaction cannot contribute significantly to exchange between the two edge fluorides (cf. above).

3. Exchange of fluoride between $UO_2(pic)F_3^{2-}$ and $UO_2(pic)F_2(H_2O)^-$ will have the same effect on the edge fluorides as exchange of the picolinate ligand. This was tested by measuring the ^{17}O-NMR spectrum of a solution of 5 mM U(VI), 20 mM picolinate, and 15 mM fluoride at pH = 6. Separate ^{17}O peaks were observed for the different complexes, at 1124.2 ppm for $UO_2(pic)F_3^{2-}$, and at 1123.0 and 1121.4 ppm for $UO_2(pic)F_2^-$ and $UO_2(pic)_2F^-$, respectively. Hence, exchange of fluoride between $UO_2(pic)F_3^{2-}$ and $UO_2(pic)F_2^-$ must be slower than the chemical shift difference of 62 Hz and cannot contribute significantly to the faster exchange between the edge fluorides.

4. Exchange between the edge fluorides can also take place through chelate ring opening followed by rotation around the remaining uranium−ligand bond and closure of the chelate ring. This process will result in a "site exchange" between coordinated N and O in the picolinate ligand, equivalent to exchange between the two edge fluorides. Ring opening is expected to be slower than the rotation and should be sensitive to substituent effects in the ligand if it involves the U(VI)−N bond. We studied this by measuring the ^{19}F-NMR spectra of ternary complexes with two substituted picolinate ligands, 4-nitropicolinate and 4-(3-pentyl)picolinate. For both, three fluorine peaks were observed for the UO_2LF_3 complexes. Their chemical shifts were close to those observed for the corresponding picolinate complex. The signal of the central fluoride was in each case a triplet with 30−40 Hz couplings, indicating that the external fluoride exchange rate is approximately the same in the three complexes. However, significant differences were observed in the line widths of the edge fluorides. In case of 4-(3-pentyl)picolinate this was 90−95 Hz, and for the 4-nitropicolinate complex 670−690 Hz. The contribution to line broadening from exchange with bulk fluoride is negligible; hence the rate constants for intramolecular exchange are 190 ± 10 s^{-1} and 1900 ± 100 s^{-1}, respectively. The larger rate constant for the 4-nitropicolinate complex is probably a result of a weaker uranium−nitrogen bond due to reduced electron density on the pyridine nitrogen atom resulting from electron withdrawal by the nitro group. In the same way the slightly lower rate observed for the 3-pentyl derivatives is consistent with the electron-donating character of the alkyl group. This supports our assumption that the rate-determining step in edge fluoride exchange is chelate ring opening via N−U(VI) bond breaking (which is still much faster than exchange between free and coordinated picolinate, where the rate-determining step seems to be dissociation of the

(21) Aas, W.; Moukhamet-Galeev, A.; Grenthe, I. Manuscript accepted for Sixth International Conference "Migration'97" Sendai, Japan.

Table 1. Pseudo-First-Order Rate Constants (s^{-1}) for Different Exchange Reactions at −5 °C

complex	$F_{coord} \leftrightarrow F_{bulk}$	$L_{coord} \leftrightarrow L_{bulk}$
$UO_2(pic)F_3^{2-}$	12.8 ± 0.3^a	4.7 ± 0.2
	24.4 ± 0.6^b	
$UO_2(ox)F_3^{3-}$	14.1 ± 0.8^a	6.2 ± 0.4
	21.6 ± 2.4^b	
$UO_2(CO_3)F_3^{3-}$	15.0 ± 2.8	5.7 ± 2.1
$UO_2(ox)F_2(H_2O)^-$	15.8 ± 1.2	
$UO_2(CO_3)F_2(H_2O)^{2-}$	14.4 ± 3.0	
$UO_2(pic)_2F^-$	12.6 ± 1.5	
$UO_2(ox)_2F^{3-}$	12.3 ± 1.0	8.7 ± 1.5
$UO_2(ac)F_3^{2-}$	∼40−50	∼2000
$UO_2(CO_3)_3^{4-}$		1.8^c
$UO_2F_5^{3-}$	43.4^d	

[a] For the edge fluorides. [b] For central fluoride. [c] By Brücher et al.[28] [d] By Tomiyasu et al.[26] (M^{-1} s^{-1}).

carboxylate group). Similar internal rotation of "hemilabile" ligands has recently been studied by multinuclear NMR.[11,22−24] However, direct observations of chelate ring opening are rare.

Structure and Dynamics in $UO_2(ox)F_3^{3-}$, $UO_2(CO_3)F_3^{3-}$, and $UO_2(ac)F_3^{2-}$. The $UO_2(ox)F_3^{3-}$ and $UO_2(CO_3)F_3^{3-}$ ions have C_{2v} symmetry, and two narrow peaks in the ratio 2:1 can be observed in their ^{19}F-NMR spectra. Spin−spin coupling between the different fluorides results in a triplet for the central, and a doublet for the two equivalent edge fluorides, with $^2J_{F,F}$ = 39 Hz for oxalate and $^2J_{F,F}$ = 28 Hz for carbonate. Exchange between free and coordinated fluoride was studied by magnetization transfer experiments as described above for the picolinate ligand. The rate constants of exchange for the different coordinated fluorides in $UO_2(ox)F_3^{3-}$ are approximately the same as in $UO_2(pic)F_3^{3-}$, the edge fluorides exchanging more slowly than the central one, k_{obs}(edge) = 14.1 ± 0.8 s^{-1} and k_{obs}(central) = 21.6 ± 2.4 s^{-1}, while in the corresponding carbonate complex there is practically no difference, k_{obs}(edge) = k_{obs}(central) = 15.0 ± 2.8 s^{-1} (Table 1).

Acetate forms much weaker complexes than both carbonate and oxalate. The equilibrium constant for reaction 6 was

$$UO_2F_3^- + ac^- \rightleftharpoons UO_2(ac)F_3^{2-} \quad (6)$$

calculated from the fluorine peak integrals and the known stability constants for the binary complexes,[25] $K \approx 10$ M^{-1}. The small value does not allow a decision to be made on whether acetate coordinates through one or two carboxylate oxygens. However, there are two fluorine NMR peaks in the ratio 2:1 in $UO_2(ac)F_3^{2-}$, which clearly indicates five-coordination and therefore a bidentate coordination of acetate. These peaks are much broader, about 700 Hz, than those in the other UO_2LF_3 complexes. This is not a result of fast exchange between free and coordinated fluoride as indicated by a fluorine magnetization transfer experiment made by inverting the free fluoride signal. The rate constant for both fluoride sites is $k_{obs1} \approx 40-50$ s^{-1}. The larger uncertainty is due to difficulty in integrating the broad lines. The rate is independent of free fluoride and acetate concentrations, indicating a mechanism with two parallel pathways (cf. Scheme 2).

The new pathway in Scheme 2 involves complete dissociation of acetate (k_{obs2}) followed by rapid exchange between coordinated and free fluoride (k_{obs3}). The rate constant for this latter

Scheme 2

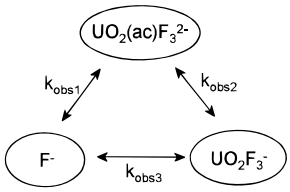

process has been reported ((4.7 ± 1.3) × 10^3 M^{-1} s^{-1}).[8] The rate-determining step is dissociation of acetate with an approximate rate constant, $k_{obs2} \approx 2000$ s^{-1}, deduced from the observed line broadening of coordinated fluoride. It was not possible to study the acetate exchange directly from the ^{1}H NMR acetate signals, because of small chemical shift differences and the high concentration of free acetate used.

Exchange between free and coordinated oxalate or carbonate was studied by ^{13}C-NMR inversion transfer experiments using ^{13}C-enriched oxalate and carbonate. A rate constant of 6.2 ± 0.4 s^{-1} was obtained for exchange between $UO_2(ox)F_3^3$ and free oxalate. A significantly higher rate constant, 17.2 ± 2.1 s^{-1}, for carbonate exchange was measured for $UO_2(CO_3)F_3^{3-}$ at pH = 7.82. This is largely due to the contribution of a fast proton-catalyzed pathway, as observed recently[12] for $UO_2(CO_3)_3^{4-}$. In order to confirm this, we varied the pH between 6.5 and 8 and measured the line width of $UO_2(CO_3)F_3^{3-}$. The dominant species in these solutions are $UO_2(CO_3)F_3^{3-}$, $UO_2(CO_3)_3^{4-}$, and free carbonate. The line width of $UO_2(CO_3)F_3^{3-}$ may therefore depend on the following processes:

$$UO_2(CO_3)F_3^{3-} \rightleftharpoons UO_2(CO_3)F_2^{2-} + F^- \quad (7)$$

$$UO_2(CO_3)F_3^{3-} \rightleftharpoons UO_2F_3^- + CO_3^{2-} \quad (8)$$

$$UO_2(CO_3)F_3^{3-} + H^+ \rightleftharpoons UO_2F_3^- + HCO_3^- \quad (9)$$

$$UO_2(CO_3)F_3^{3-} + H^+ \rightleftharpoons UO_2(CO_3)F_2^{2-} + HF \quad (10)$$

In the investigated pH range we found a linear relationship between the rate of carbonate exchange and the hydrogen ion concentration (Supporting Information, S3). From the slope of a least-squares fitted line, a rate constant of (7.6 ± 0.5) × 10^8 M^{-1} s^{-1} was calculated for the proton-catalyzed carbonate dissociation, eq 9. Hence the contribution of this process to the rate constant for carbonate exchange, measured at pH = 7.82 by ^{13}C magnetization transfer, is approximately 11.5 s^{-1}. The rate constant of dissociation of carbonate as given by eq 8 is the difference between these two values, 5.7 ± 2.1 s^{-1}, *i.e.*, close to the rate constant for exchange of oxalate and picolinate in these complexes. The intercept 27.2 ± 3.9 s^{-1} represents the sum of the rate constants for dissociation of fluoride and carbonate (eqs 7 and 8). Using the above rate constant for eq 8, we obtain a rate constant of 21.5 ± 5.9 s^{-1} for the dissociation of fluoride, eq 7. This value is in fair agreement with the fluoride exchange rate constant obtained in the ^{19}F inversion transfer experiment, at pH = 6.83, mentioned above (15.0 ± 2.8 s^{-1}). The contribution of proton-catalyzed fluoride exchange (eq 10) is therefore negligible in this pH region.

Structure and Dynamics in UO_2L_2F. Three isomers are possible for the picolinate complex (Figure 2), but only one peak, at 178.3 ppm, was observed in the ^{19}F-NMR spectrum. This could be a result of fast exchange between the isomers and free fluoride, but magnetization transfer experiments showed that such exchange was slow, 12.6 ± 1.5 s^{-1}. Alternatively, exchange could take place via internal rotation of coordinated

(22) Fokken, S.; Spaniol, T. P.; Kang, H.; Massa, W.; Okuda, J. *Organometallics* **1996**, *15*, 5069.
(23) Sakharov, S. G.; Zarelua, S. A.; Kokunov, Y. V.; Buslaev, Y. A. *Inorg. Chem.* **1992**, *31*, 3302.
(24) Sakharov, S. G.; Buslaev, Y. A.; Tkac, I. *Inorg. Chem.* **1996**, *35*, 5514.
(25) Ahrland, S.; Kullberg, L. *Acta Chem. Scand.* **1971**, *25*, 3457−3470.

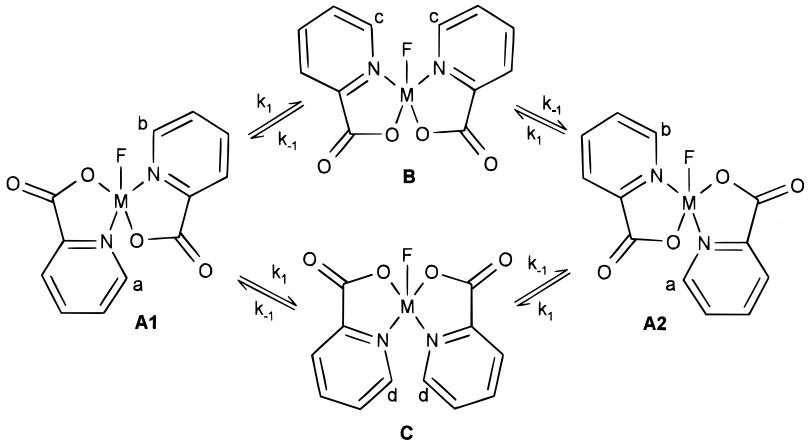

Figure 2. Isomers of and intramolecular exchange pathways for $UO_2(pic)_2F^-$.

picolinate, as described above. It was not possible to "freeze out" the different isomers in aqueous solution; in CD_3OD at −54 °C (prepared by dissolving solid $Na[UO_2(pic)_2F]$) two fluoride signals and two sets of proton signals were observed, indicating the presence of two isomers under these conditions (Supporting Information, S5). The cross peaks in the phase-sensitive proton 2D-EXSY spectrum (Supporting Information, S6) show exchange between the H-6 atoms of the two pyridine rings, and Figure 2 demonstrates exchange of the magnetically nonequivalent protons of the major isomer (**A1** and **A2** are structurally equivalent) with the similar magnetically equivalent protons of a minor isomer (**B** or **C**). The cross peaks in the latter spectrum (Supporting Information, S6), resulting from NOE, were used for assigning these protons, and this assignment was in accordance with the 2D COSY spectrum. Only two of the three possible isomers shown in Figure 2 were identified, and it is assumed that the minor symmetrical isomer is **B**. The third isomer, **C**, which has all of the negatively charged groups adjacent to one another, is considered to be less stable and not observed. Clearly the isomerization reaction is *intramolecular*, and we assume that the findings in CD_3OD are also valid in aqueous solutions. From 1D proton spectra, measured in the temperature range −54 to −90 °C, it was possible to integrate the separate proton signals for the two isomers and to calculate the equilibrium constant as a function of temperature, giving $\Delta H° = 4.9 \pm 0.3$ kJ mol^{-1} (Supporting Information, S7). From this the equilibrium constant $K(-5\ °C) = [\mathbf{B}]/[\mathbf{A}]$, ($[\mathbf{A}] = [\mathbf{A1}] + [\mathbf{A2}]$) was calculated as approximately 0.5. From the measured line widths and the calculated populations, the exchange rates at different temperatures were also calculated,[20] giving $\Delta H^‡ = 26.9 \pm 0.5$ kJ mol^{-1} and $\Delta S^‡ = 82.9 \pm 0.6$ J mol^{-1} K^{-1} (Supporting Information, S8). A comparison between measured and calculated spectra obtained using these data is given in the Supporting Information (S9). The internal rotation rate constant at −5 °C is calculated to be approximately 1500 s^{-1}, which is 5 times larger than the value obtained for $UO_2(pic)F_3^{2-}$. There is only one isomer of $UO_2(ox)_2F^{3-}$, and only one narrow peak (at 146.1 ppm) was observed in the fluorine spectrum. The pseudo-first-order rate constant for exchange between coordinated and free fluoride, as measured by inversion transfer, was 12.3 ± 1.0 s^{-1}. This value is approximately equal to the fluoride rate constant of exchange for the edge fluorides in $UO_2OxF_3^{3-}$. The exchange rate constant with oxalate was determined by ^{13}C-NMR inversion transfer experiments as 8.7 ± 1.5 s^{-1}. This value is close to the exchange rate constant for exchange of oxalate in $UO_2(ox)F_3^{3-}$ as discussed above.

Structure and Dynamics in $UO_2LF_2(H_2O)$. There are three different isomers and six magnetically different fluoride sites

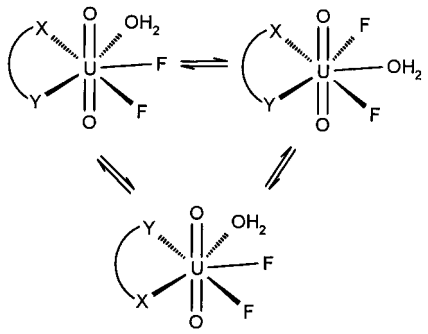

Figure 3. Isomers of $UO_2LF_2(H_2O)$.

in $UO_2(pic)F_2(H_2O)^-$ (Figure 3; X = N, Y = O). However, only three fluoride peaks were observed, two at about 155 and 160 ppm and the third under the $UO_2(pic)F_3^{2-}$ peak at 144.6 ppm. The reason for finding three peaks instead of six is probably a result of small chemical shift differences between fluorides in similar chemical surroundings in the three isomers. The observed peaks were very broad compared to signals for complexes with no coordinated water, indicating another exchange pathway for the fluorides as discussed below. The ratio of the observed intensities, 1:1.5:2, differs from the expected ratio 2:2:2, reflecting small differences in thermodynamic stability between the isomers.

There are three different fluorides in the two isomers of $UO_2(ox)F_2(H_2O)^{2-}$ and $UO_2(CO_3)F_2(H_2O)^{2-}$ (Figure 3; X = Y = O). Statistically one expects twice as much of the unsymmetrical isomer, resulting in a 1:1:1 ratio for the different fluoride peaks. Three broad peaks are observed in the ^{19}F-NMR spectrum of $UO_2(ox)F_2(H_2O)^{2-}$ (Figure 4), confirming the existence of two isomers. One peak, probably from the symmetrical isomer at 134 ppm, is about 1.5 times higher than the other two, indicating a stability difference between the isomers similar to that observed for the picolinate complex. In the ^{19}F-NMR spectrum of the corresponding carbonate complex only two broad peaks, with an intensity ratio 2:1, were observed (133 and 140 ppm). The 133 ppm peak is probably the result of two overlapping peaks with similar chemical shifts (see Supporting Information, S10).

The rate constant for exchange between free and coordinated fluoride, studied by magnetization transfer, was 15.8 ± 1.2 s^{-1} for $UO_2(ox)F_2(H_2O)^{2-}$ and 14.4 ± 3.0 s^{-1} for $UO_2(CO_3)F_2(H_2O)^{2-}$, *i.e.*, very close to the values observed for $UO_2LF_3^{3-}$. Hence the observed broad lines cannot be due to exchange with free fluoride or oxalate/carbonate, because these rates are too slow to affect the line width. The most likely reason for the broadness is site exchange between coordinated

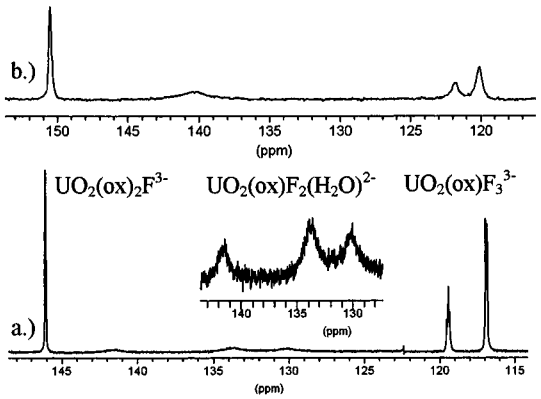

Figure 4. ^{19}F-NMR spectra of a solution containing 5 mM UO_2^{2+}, 10 mM oxalate, and 20 mM fluoride, pH = 6.5 (a) at −5 °C and (b) at 25 °C. The free fluoride signal at around 0 ppm is not shown. (See details in the text.)

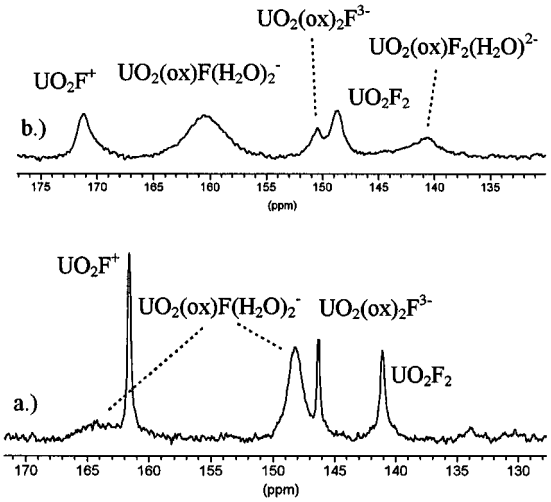

Figure 5. ^{19}F-NMR spectra of a solution containing 5 mM UO_2^{2+}, 5 mM oxalate, and 3 mM fluoride at pH = 4.4 (a) at −5 °C and (b) at 25 °C. They show the existence of two isomers of $UO_2(ox)F(H_2O)_2^-$.

water and fluoride, taking place via exchange with external water. The rate constant estimated from the line broadening is approximately 1600 s^{-1}, which is 2 orders of magnitude slower than water exchange for the hydrated uranyl ion at the same temperature.[26] Precise data could not be obtained for the corresponding picolinate complex because of overlapping fluoride peaks.

There are few studies of variations in the rate of exchange of coordinated water in binary (or ternary) complexes $M(H_2O)_pL_q$ is varied. The main reason for this is the experimental difficulties associated with studying reactions of this type using the traditional methods of fast kinetics. Fukutomi et al.[26] have investigated the water exchange in the ternary $UO_2^{2+}-H_2O-$DMSO system and found that the coordination of DMSO resulted in a decrease in rate by 1 order of magnitude.

Structure and Dynamics in $UO_2LF(H_2O)_2$. We were only able to obtain information for the oxalate system. In a solution of 5 mM U(VI), 5 mM oxalate, and 3 mM fluoride at pH = 4.4 and −5 °C, $UO_2(ox)F(H_2O)_2^-$ is the dominant species present, and two broad peaks, one at 148.1 ppm and the other at about 163−165 ppm, are observed in the ^{19}F spectrum; these peaks coalesce at 25 °C (Figure 5). This information is consistent with the presence of both of the two possible isomers, Figure 6. The narrow lines observed for the other complexes present

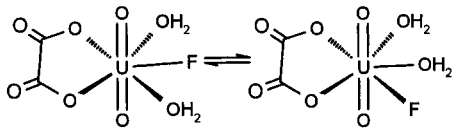

Figure 6. Isomers observed for $UO_2(ox)F(H_2O)_2^-$.

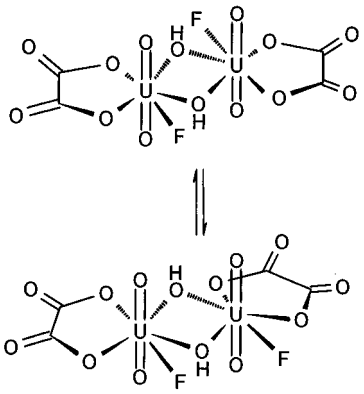

Figure 7. Hydroxide-bridged isomers of $(UO_2)_2(ox)_2F_2(OH)_2^{4-}$.

in solution (including the binary complexes) indicate that exchange between them does not involve the binary complexes, or external fluoride, but occurs via slow water exchange of the type mentioned above. The rate constant for exchange of coordinated water is estimated at 1800 s^{-1} using the line width (590−600 Hz) of the major isomer ($k = \pi\Delta\nu_{1/2(obs)}$), *i.e.*, close to the value for $UO_2(ox)F_2(H_2O)^{2-}$.

Structure and Equilibrium Constant for $(UO_2)_2(ox)_2F_2(OH)_2^{4-}$. By increasing the pH of solutions 5 mM in uranium(VI), 30 mM fluoride, 10 mM oxalate, at −5 °C, we observed two narrow singlets in the fluorine spectrum at 128.07 and 128.32 ppm (in addition to signals for $UO_2(ox)F_3^{3-}$, $UO_2(ox)_2F^{3-}$, and $UO_2(ox)F_2^{2-}$). Their intensities and line widths were the same and increased with increasing pH, until precipitation occured at pH = 8.3. From the reaction stoichiometry and the strong tendency of uranium(VI) to form hydroxide-bridged polynuclear complexes,[27,28] we suggest that the peaks refer to the two dimeric isomers shown in Figure 7. In order to check this, the stability constant for reaction eq 11 was estimated from the peak integrals. From these values,

$$2UO_2(ox)F^- + 2H_2O \rightleftharpoons (UO_2)_2(ox)_2F_2(OH)_2^{4-} + 2H^+ \quad (11)$$

obtained at different concentrations of reactants and at different values of pH, a constant value log $K = -11.9$ was obtained. From the known stability constant for the formation of $UO_2(ox)F^-$, the value log $\beta = 7.9$ was obtained for reaction 12. The fluoride peaks coalesce at 25 °C, indicating fast

$$2UO_2^{2+} + 2ox^{2-} + 2F^- + 2H_2O \rightleftharpoons (UO_2)_2(ox)_2F_2(OH)_2^{4-} + 2H^+ \quad (12)$$

exchange between the isomers. We did not study the kinetics of this exchange because of the very low concentration of the isomers. However, we suggest that it occurs via fluoride dissociation in the dimer rather than via cleavage of a hydroxide bridge.

(26) Ikeda, Y.; Soya, S.; Fukutomi, H.; Tomiyasu, H. *J. Inorg. Nucl. Chem.* **1979**, *41*, 1333.

(27) Grenthe, I.; Fuger, J.; Konings, R. J. M.; Lemire, R. J.; Muller, A. B.; Nguyen-Trung, C.; Wanner, H. *Chemical Thermodynamics of Uranium*; North-Holland: Amsterdam, 1992; Vol. 1.

(28) Brücher, E.; Glaser, J.; Tóth, I. *Inorg. Chem.* **1991**, *30*, 2239−2941.

Acknowledgment. We are grateful to the Swedish Institute and to Franz Georg och Gull Liljenroth's Stiftelse for research fellowships covering Z.Sz.'s stay in Stockholm. Dr. Kingsley J. Cavell (University of Tasmania, Australia), Dr. Ferenc Kóródi (ICN-Alkaloida, Hungary), and Ms. Maria J. Gonzalez (KTH, Sweden) are thanked for providing us with some ligands.

Supporting Information Available: Listings of equilibrium constants, log β_{pq}, for the reactions $UO_2^{2+} + pL + qF^- \rightleftharpoons UO_2L_pF_q$ (T1), ^{1}H-NMR spectrum (S2) and ^{19}F and ^{1}H selective magnetization transfer results (S1, S3) for $UO_2(pic)F_3^{2-}$, line width dependence of the ^{13}C-NMR signal of $UO_2(CO_3)F_3^{3-}$ on pH (S4), ^{1}H-NMR spectra (S5), ^{1}H 2D-EXSY (S6), temperature dependence of the equilibrium constant (S7) and the rate constant (S8), and calculated and measured temperature dependent ^{1}H-NMR spectra (S9) for $UO_2(pic)_2F^-$, and ^{19}F-NMR spectrum (S10) of $UO_2(CO_3)F_2(H_2O)^{2-}$ (10 pages). Ordering information is given on any current masthead page.

IC9708172